NUKLEONIKA 2013;58(1):57–61

ORIGINAL PAPER

X-ray diffraction, Mössbauer spectroscopy, and magnetoelectric effect studies of $(BiFeO_3)_x$-$(BaTiO_3)_{1-x}$ solid solutions

Karol Kowal, Elżbieta Jartych, Piotr Guzdek, Paweł Stoch, Beata Wodecka-Duś, Agata Lisińska-Czekaj, Dionizy Czekaj

Abstract. In this work the hyperfine interactions in $(BiFeO_3)_x$-$(BaTiO_3)_{1-x}$ solid solutions with relation to their structural properties have been investigated. X-ray diffraction, Mössbauer spectroscopy and magnetoelectric effect measurements have been used for studies of sintered $(BiFeO_3)_x$-$(BaTiO_3)_{1-x}$ solid solutions with x = 0.9, 0.8 and 0.7. With increasing contents of $BaTiO_3$, the structural transformation from rhombohedral to cubic was observed. The weakening of the hyperfine magnetic fields accompanied by this transformation. On the other hand, the increasing amount of $BaTiO_3$ caused an increase of the magnetoelectric effect.

Key words: multiferroics • hyperfine interactions • Mössbauer spectroscopy • magnetoelectric effect

K. Kowal✉
National Centre for Nuclear Research,
Nuclear Energy Division,
7 Andrzeja Sołtana Str., 05-400 Otwock/Świerk, Poland,
Tel.: +48 22 718 0126, Fax: +48 22 779 3481,
E-mail: k.kowal@ncbj.gov.pl

E. Jartych
Lublin University of Technology,
Institute of Electronics and Information Technology,
38A Nadbystrzycka Str., 20-618 Lublin, Poland

P. Guzdek
Institute of Electron Technology, Cracow Division,
39 Zabłocie Str., 30-701 Kraków, Poland

P. Stoch
National Centre for Nuclear Research,
7 Andrzeja Sołtana Str., 05-400 Otwock/Świerk, Poland
and AGH University of Science and Technology,
Faculty of Materials Science and Ceramics,
al. A. Mickiewicza 30, 30-059 Krakow, Poland

B. Wodecka-Duś, A. Lisińska-Czekaj, D. Czekaj
University of Silesia,
Institute of Materials Science,
2 Śnieżna Str., 41-200 Sosnowiec, Poland

Received: 5 July 2012
Accepted: 14 September 2012

Introduction

Bismuth ferrite, $BiFeO_3$, is the most investigated multiferroic material in which ferroelectricity coexists with an antiferromagnetic order at room temperature. The crystalline structure of $BiFeO_3$ is well recognized for monocrystals as well as for polycrystalline materials or thin films. $BiFeO_3$ is reported to have a rhombohedrally distorted perovskite-like structure ABO_3. The unit cell has parameters a = 3.96 Å and α = 89°28' when described by the space group $R3c$ [1] or a = 5.58102(4) Å and c_{hex}= 13.8757(2) Å in the hexagonal setting [10]. For this compound, the ferroelectric Curie temperature T_C = 1103 K and the antiferromagnetic Néel temperature T_N = 643 K [13, and references therein]. The ferroelectric polarization is caused by the shifts of Fe^{3+}, Bi^{3+} and O^{2-} ions from their centrosymmetrical positions. The magnetic ordering of $BiFeO_3$ at room temperature is a combination of antiferromagnetic G-type ordering with spiral modulation of spins of 620 Å period [10]. The coexistence of ferroelectric and antiferromagnetic properties in $BiFeO_3$ creates the possibility for many applications of this material and $BiFeO_3$-type compounds, amoung others in systems to steering the magnetic memory by electric field and, *vice versa*, in microelectronics, spintronics and sensor technique [17].

As neutron-scattering experiments showed, in $BiFeO_3$ the superexchange interaction produce a canted antiferromagnetic order, where the spin-up and spin-down sublattices are not strictly parallel, causing a weak ferromagnetism [15]. In the bulk material, the spiral ordering is superimposed rendering $BiFeO_3$ paramagnetic. Recently, the aim of investigations on bismuth ferrite is to suppress the spiral spin structure in order to release the inherent magnetization and, in consequence, to improve its multiferroic properties [11]. One of the way to destroy the spiral structure is a structural modification or deformations introduced by cation substitutions or doping. As recently reported in [11], the addition of ferroelectric $BaTiO_3$ compound in order to obtain $BiFeO_3$-$BaTiO_3$ solid solution allowed to release the latent magnetization locked within the spiral spin structure what was confirmed by the magnetization studies. Moreover, the presence of magnetoelectric coupling in $BiFeO_3$-$BaTiO_3$ solid solution was also reported in some papers [8, 9].

In this work the solid solutions of $(BiFeO_3)_x$-$(BaTiO_3)_{1-x}$, marked later as $(BFO)_x$-$(BTO)_{1-x}$, were successfully prepared by a solid-state reaction. The aim of these investigations was to determine the structure, hyperfine interactions and the magnitude of magnetoelectric effect in these materials depending on the chemical composition. X-ray diffraction (XRD), Mössbauer spectroscopy (MS) and measurements of magnetoelectric effect (ME) were used as research methods.

Experimental details

The investigated $(BFO)_x$-$(BTO)_{1-x}$ solid solutions were prepared from constituents of 99.9% purity. For various x values, i.e. 0.9, 0.8 and 0.7, the solid-state sintering method, described elsewhere in [16], was used in accordance with the stoichiometric requirements presented below:

$$(1)\quad (Bi_2O_3)_{x/2} + (Fe_2O_3)_{x/2} + (BaCO_3)_{1-x} + (TiO_2)_{1-x} \rightarrow (BiFeO_3)_x - (BaTiO_3)_{1-x} + (CO_2)_{1-x}$$

The supplied ceramic powders were mixed in a 96% ethanol solution by 24 h, using a mill with zirconia balls, in order to ensure high homogeneity of the considered materials and maximize the grains fragmentation. The resulting mixture was then placed into steel matrices and pressed to form disks with a diameter of 10 mm and 1 mm thickness. For this purpose, the hydraulic press, providing pressure of 300 MPa, has been used. The prepared compacts were stacked in alumina crucibles and sintered in an electric chamber furnace Termod KS-1350 with a linear (150 $K \cdot h^{-1}$) and programmable increase in temperature. The double syntheses at the temperature $T = 1073$ K during the time $t = 10$ h and the final sintering at 1103 K during 20 h have been applied. After that, the ceramics were annealed in air at a temperature of 823 K for 10 h and then cooled with a linear (100 $K \cdot h^{-1}$) decrease in temperature.

The crystalline structure of the sintered $(BFO)_x$-$(BTO)_{1-x}$ solid solutions was examined using a Philips PW3710 diffractometer with CoK_α radiation. The phase and structural analysis of the recorded X-ray patterns was performed with an X'Pert High Score Plus computer program equipped with the newest ICSD data base and the Rietveld method of the crystalline structure refinement.

MS studies were carried out at room temperature in standard transmission geometry using a source of ^{57}Co in a chromium matrix. Tablets of investigated solid solutions were crushed and powdered in a mortar, the absorbers were prepared using a self-adhesive transparent foil. A 25-μm-thick metallic iron foil was taken as a standard for calibration of a spectrometer.

The magnetoelectric effect was measured on the solid tablets at room temperature by the dynamic lock-in method, which has been described previously in the literature [4]. The samples were placed in a DC magnetic field created by an electromagnet and AC sinusoidal magnetic field produced by Helmholtz coils. The applied DC and AC fields were perpendicular to the sample surface. The induced voltage between sample surfaces was measured with a lock-in amplifier (Stanford Research System, model SR 830) with an input resistance of 100 MΩ and a capacitance of 25 pF. The lock-in amplifier was used in differential mode. To measure the DC and AC magnetic field, a Hall probe SM 102 was applied. Magnetoelectric coefficients α_{ME} were determined for various magnitudes of the DC static magnetic field (0.1–4.5 kOe).

Results and discussion

As reported in the literature, the crystallographic symmetry of $(BFO)_x$-$(BTO)_{1-x}$ solid solutions changes from rhombohedral for $0.67 < x < 1$ to cubic for $0.07 < x < 0.67$ and finally, to tetragonal for $x < 0.07$ [2, 5] (Fig. 1).

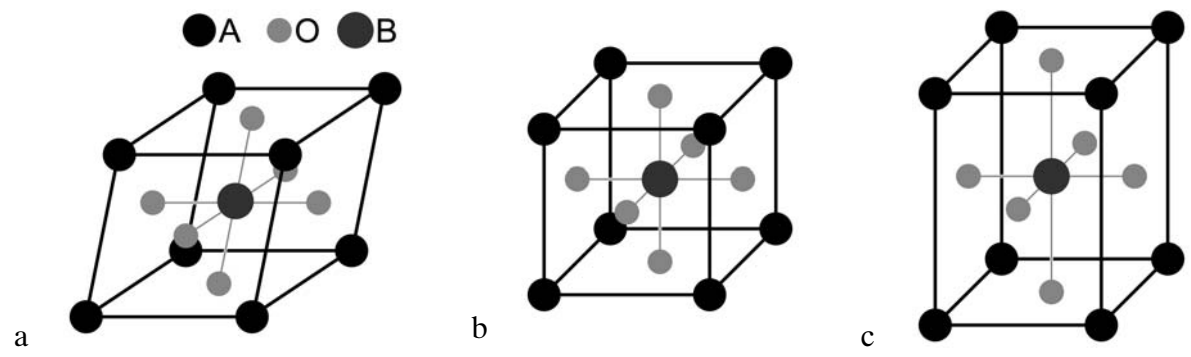

Fig. 1. The unit cells of perovskite-like structure ABO_3: (a) rhombohedrally distorted, (b) cubic and (c) tetragonal; A positions are occupied by Bi^{3+} and Ba^{2+} ions; B positions are occupied by Fe^{3+} and Ti^{4+} ions.

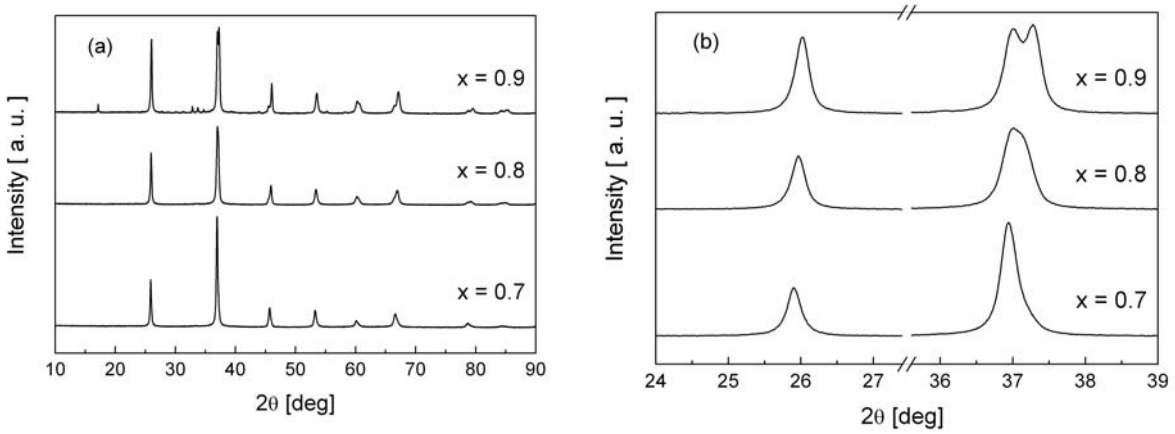

Fig. 2. X-ray diffraction patterns of $(BFO)_x$-$(BTO)_{1-x}$ solid solutions in dependence on x (CoK_α radiation was used); (a) full pattern; (b) expanded view of XRD of two more intensive lines.

Small amount of $BaTiO_3$ stabilizes the perovskite structure of $BiFeO_3$. The results of XRD measurements for the $(BFO)_x$-$(BTO)_{1-x}$ solid solutions studied in this work are presented in Fig. 2. In the case of $x = 0.9$, the phase and structural analysis proved that the weight fraction of $BiFeO_3$ was about 83.3%, while that for $BaTiO_3$ was about 10.5%. The rest 6.2% comes from $Bi_2Fe_4O_9$ impurity. The lattice parameters calculated from the patterns are as follows: $a = b = 5.5949(1)$ Å, $c = 13.8709(5)$ Å, $\alpha = \beta = 90°$, $\gamma = 120°$ (space group $R3c$) for $BiFeO_3$, and $a = 3.9743(4)$ Å, $b = 5.5757(7)$ Å, $c = 5.6523(6)$ Å, $\alpha = \beta = \gamma = 90°$ (space group $Amm2$) for $BaTiO_3$. The obtained results agree well with the data reported for $(BFO)_x$-$(BTO)_{1-x}$ solid solutions prepared using the molten salt method [11]. The evolution of the XRD patterns shows phase transformation from rhombohedral, when $x = 0.9$ to cubic when $x = 0.7$. The evidence of this transformation is the shift of diffraction lines to a lower two-theta angle and the conversion of double peak near 37.5°(for $x = 0.9$) into one peak near 37° (for $x = 0.7$) (see Fig. 2b). For cubic phase, the lattice constants are as follows $a = b = c = 3.9853(1)$ Å, and $\alpha = \beta = \gamma = 90°$ and they are in good agreement with parameters for the $(BFO)_x$-$(BTO)_{1-x}$ solid solutions prepared by the molten salt method [11]. The sample with $x = 0.8$ seems to be a mixture of two phases, i.e. rhombohedral and cubic with the weight fraction of about 70 and 30%, respectively. For all the samples, the average crystallite sizes are of the order of 300 Å, while the mean level of internal stress is about 0.1%.

Mössbauer spectra of $(BFO)_x$-$(BTO)_{1-x}$ solid solutions are shown in Fig. 3. It may be seen that the spectra are superposition of the quadrupolar and magnetic components. The best numerical fitting of the spectra was obtained applying the distribution of magnetic fields with a fixed quadrupole doublet. The hyperfine interactions parameters of the quadrupolar component are as follows: the isomer shift $\delta = 0.35$ mm·s^{-1} and the quadrupole splitting $\Delta = 0.26$ mm·s^{-1} (with the half width at half maximum of spectral lines $\Gamma = 0.22$ mm·s^{-1}). As the contents of $BaTiO_3$ increases in the solid solutions, the spectra become broadened reflecting the disorder in the superexchange magnetic interactions resulting from the random distribution of Fe^{3+} ions which may substitute Ti^{4+} ions within the structure of $(BFO)_x$-$(BTO)_{1-x}$ solid solutions. The hyperfine magnetic field distributions for the studied solid solutions are presented in Fig. 4. It may be noted that the average value of the hyperfine magnetic field induction decreases from $<B_{hf}> = 46.8$ T for $x = 0.9$, by $<B_{hf}> = 43.7$ T for $x = 0.8$ down to $<B_{hf}> = 39.0$ T for $x = 0.7$. The obtained results reflect the weakening of the inherent strength of the magnetic interactions associated with increasingly

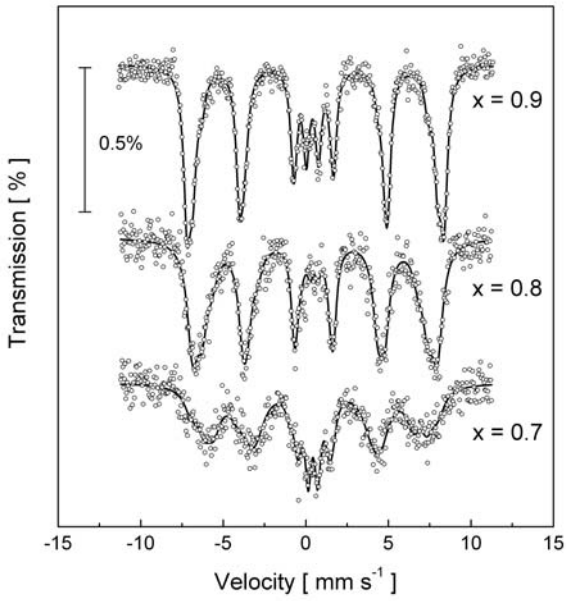

Fig. 3. Room-temperature Mössbauer spectra of $(BFO)_x$-$(BTO)_{1-x}$ solid solutions in dependence on x.

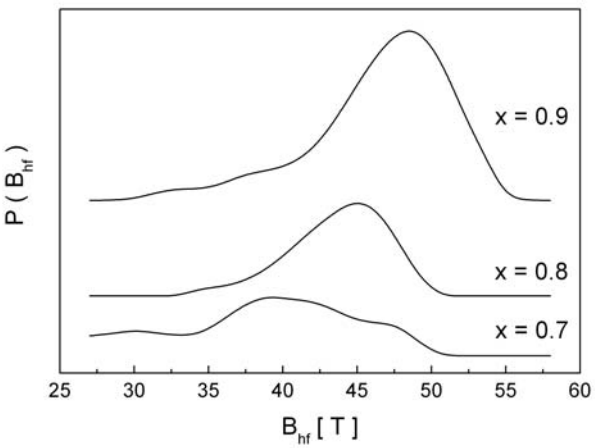

Fig. 4. Hyperfine magnetic field distributions for $(BFO)_x$-$(BTO)_{1-x}$ solid solutions in dependence on x.

spin disordering. Our results are in good agreement with the data reported for the $(BFO)_x$-$(BTO)_{1-x}$ solid solutions prepared by the molten salt method (i.e. $<B_{hf}>$ = 47.7 T for $x = 0.9$, $<B_{hf}>$ = 43.9 T for $x = 0.8$ and $<B_{hf}>$ = 40.6 T for $x = 0.7$) [11].

It is worth adding that the relative contribution of the doublet component estimated from the area of the spectrum is about 12% for $x = 0.9$, 3% for $x = 0.8$ and 13% for $x = 0.7$. This observation may have connection with the structural transformation and coexistence of two various crystallographic lattices for $x = 0.8$. The values of the hyperfine interactions parameters for the doublet mentioned above are in good agreement with a similar doublet in the spectra of $(BFO)_x$-$(BTO)_{1-x}$ solid solution for $x = 0.5$ prepared by the molten salt method (i.e. $\delta = 0.31$ mm·s^{-1} and $\Delta = 0.25$ mm·s^{-1}) [11]. It suggests that the doublet may be attributed to the cubic phase. On the other hand, one may suppose that the doublet could belong to the impurity phase like $Bi_2Fe_4O_9$, which is easily formed during synthesis because of strong evaporation of Bi. However, the hyperfine interactions parameters reported for $Bi_2Fe_4O_9$ in [7] are significantly different than those determined in this study, namely the authors measured two doublets for this compound with $\delta_1 = 0.24$ mm·s^{-1}, $\Delta_1 = 0.36$ mm·s^{-1} for the first doublet and $\delta_2 = 0.12$ mm·s^{-1}, $\Delta_2 = 0.94$ mm·s^{-1} for the second one.

As suggested in the literature, adding of $BaTiO_3$ destroy the spiral magnetic structure of the $BiFeO_3$ leading to the occurrence of linear magnetoelectric effect [12, 13]. The ME effect, which is defined as an induced dielectric polarization under the applied magnetic field, is generally characterized by the magnetoelectric voltage coefficient α_{ME}:

$$\alpha_{ME} = V/(H_{AC} \cdot d) \tag{2}$$

where V is the voltage generated due to magnetoelectric effect, H_{AC} is the amplitude of the sinusoidal magnetic field and d is the thickness of the sample. Measurements of the magnetoelectric coefficient α_{ME} were performed by recording the voltage output (V) as a function of bias magnetic field H_{DC} and frequency of sinusoidal magnetic field H_{AC}. The α_{ME} coefficient was calculated from the voltage output following the relation (2). The results of the measurements for various magnitudes of the DC static magnetic field are presented in Fig. 5.

As seen in Fig. 5, the magnitude of ME effect for a given value of H_{DC} increases with increasing $BaTiO_3$ content. Simultaneously, the α_{ME} value decreases with increasing value of DC magnetic field for all samples studied in this work. The obtained results do not agree with the data reported for similar $(BFO)_x$-$(BTO)_{1-x}$ solid solutions, where the ME output increased with increasing DC field, reaching a maximum at 5.5. kOe and later decreased [8, 9]. This discrepancy may be explained by the fact that in our case the samples were not poled electrically and magnetically before the main ME measurements and the AC field (5 Oe) applied was much smaller than that reported in [8, 9] (18 Oe). On the other hand, the similar dependence, as observed by us, was previously reported for $BaTiO_3$ and ferrite solid solutions [6] and in some Aurivillius phases [9]. The differences of the α_{ME} coefficients values may be attributed to the difference in composition, structure,

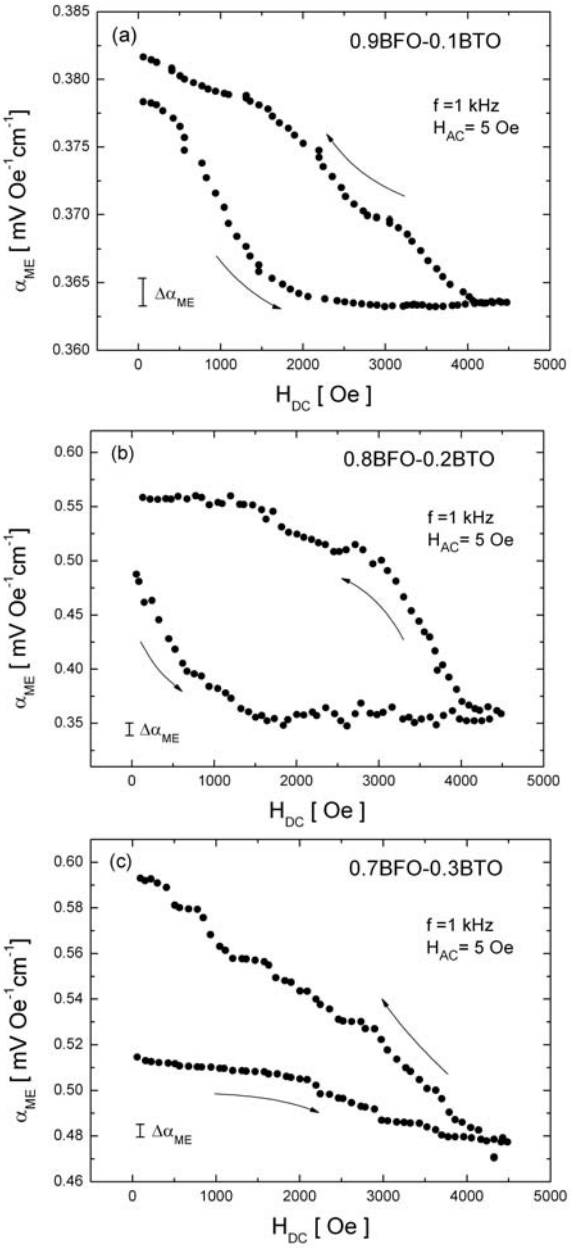

Fig. 5. Variation of magnetoelectric coefficient α_{ME} with DC bias magnetic field for $(BFO)_x$-$(BTO)_{1-x}$ solid solutions with: (a) $x = 0.9$, (b) $x = 0.8$ and (c) $x = 0.7$; the uncertainty $\Delta\alpha_{ME}$ of magnetoelectric voltage coefficient has the same value for the respective data.

preparation conditions, microstructure or measuring methods as was previously described in [3]. It may be noted that for all the samples the curves do not retrace the same path on reversal magnetic field. The hysteretic nature of the $\alpha_{ME}(H_{DC})$ dependence may be due to hysteresis behavior of the solid solution constituents, e.g. in $BaTiO_3$ there was observed the electrical polarization remanence and the charge accumulation on the grain boundaries [14].

Conclusions

Employing the solid-state sintering technology, solid solutions of $(BiFeO_3)_x$-$(BaTiO_3)_{1-x}$ were prepared with different contents of $BaTiO_3$. Structural transformation

from rhombohedral to the cubic crystallographic system was observed for $x = 0.7$, while the solid solution with $x = 0.8$ seems to be a mixture of these two systems. Room-temperature Mössbauer spectra showed composition-dependent characteristic of decreasing hyperfine magnetic field. It means a gradual magnetic phase transformation from a more-ordered spin structure for $x = 0.9$ to an increasingly spin disordered magnetic phase for $x = 0.7$. Simultaneously, the collapsed quadrupole doublet may indicate the superparamagnetic relaxation due to the small particle sizes of the investigated solid solutions. The preliminary results of magnetoelectric effect also showed the dependence of α_{ME} on the $BaTiO_3$ contents. The observed irreversibility in the ME output vs. DC magnetic field may be caused by the hysteretic nature of the electrical and/or magnetic polarization of the investigated solid solutions.

Acknowledgment. The authors would like to thank Prof. J. Pszczoła from the AGH University of Science and Technology, Faculty of Physics and Applied Computer Science for his interest and fruitful discussion on the subject of this work.

References

1. Blaauw C, van der Woude F (1973) Magnetic and structural properties of $BiFeO_3$. J Phys C: Solid State Phys 6:1422–1431
2. Chandarak S, Unruan M, Sareein T *et al.* (2009) Fabrication and characterization of (1–x)$BiFeO_3$-x$BaTiO_3$ ceramics prepared by a solid state reaction method. J Magnetics 14;3:120–123
3. Duong GV, Groessinger R (2007) Effect of preparation conditions on magnetoelectric properties of $CoFe_2O_4$--$BaTiO_3$ magnetoelectric composites. J Magn Magn Mater 316:e624–e627
4. Duong GV, Groessinger R, Schoenhart M, Bueno--Basques D (2007) The lock-in technique for studying magnetoelectric effect. J Magn Magn Mater 316:390–393
5. Ismailzade IH, Ismailov RM, Alekberov AI, Salaev FM (1981) Investigation of the magnetoelectric (ME)H effect in solid solutions of the systems $BiFeO_3$-$BaTiO_3$ and $BiFeO_3$-$PbTiO_3$. Phys Status Solidi A 68:K81–K85
6. Lokare SA, Devan RS, Chougule BK (2008) Structural analysis and electrical properties of ME composites. J Alloys Compd 454:471–475
7. MacKenzie KJD, Dougherty T, Barrel J (2008) The electronic properties of complex oxides of bismuth with the mullite structure. J Eur Ceram Soc 28:499–504
8. Mahesh Kumar M, Srinivas A, Kumar GS, Suryanarayana SV (1999) Investigation of the magnetoelectric effect in $BiFeO_3$-$BaTiO_3$ solid solutions. J Phys: Condens Matter 11:8131–8139
9. Mahesh Kumar M, Srinivas A, Suryanarayana SV, Kumar GS, Bhimasankaram T (1998) An experimental setup for dynamic measurement of magnetoelectric effect. Bull Mater Sci 21;3:251–255
10. Palewicz A, Szumiata T, Przeniosło R, Sosnowska I, Margiolaki I (2006) Search for new modulations in the $BiFeO_3$ structure: SR diffraction and Mössbauer studies. Solid State Commun 140:359–363
11. Park TJ, Papaefthymiou GD, Viescas AJ, Lee Y, Zhou H, Wong SS (2010) Composition-dependent magnetic properties of $BiFeO_3$-$BaTiO_3$ solid solution nanostructures. Phys Rev B 82:024431 (10 pp)
12. Przeniosło R, Palewicz A, Regulski M, Sosnowska I, Ibberson RM, Knight KS (2006) Does the modulated magnetic structure of $BiFeO_3$ change at low temperatures? J Phys: Condens Matter 18:2069–2075
13. Ruette B, Zvyagin S, Pyatakov AP *et al.* (2004) Magnetic field-induced phase transition in BiFeO3 observed by high-field electron spin resonance: Cycloidal to homogeneous spin order. Phys Rev B 69:064114 (7 pp)
14. Singh RS, Bhimasankaram T, Kumar GS, Surayanarayama SV (1994) Dielectric and magnetoelectric properties of $Bi_5FeTi_3O_{15}$. Solid State Commun 91:567–569
15. Sosnowska I, Peterlin-Neumaier, Steichele E (1982) Spiral magnetic ordering in bismuth ferrite. J Phys C: Solid State Phys 15:4835–4846
16. Wodecka-Duś B, Czekaj D (2010) Synthesis, crystal structure and dielectric behaviour of 0.7$BiFeO_3$-0.3$BaTiO_3$ ceramics. Materiały Ceramiczne 62;2:121–125 (in Polish)
17. Zvezdin AK, Logginov AS, Meshkov GA, Pyatakov AP (2007) Multiferroics: promising materials for microelectronics, spintronics, and sensor technique. Bull Russ Acad Sci: Physics 71;11:1561–1562